AJNR

In Vivo Evaluation of Quantitative MR Angiography in a Canine Carotid Artery Stenosis Model

M. Calderon-Arnulphi, S. Amin-Hanjani, A. Alaraj, M. Zhao, X. Du, S. Ruland, X.J. Zhou, K.R. Thulborn and F.T. Charbel

In Vivo Evaluation of Quantitative MR Angiography in a Canine Carotid Artery Stenosis Model

M. Calderon-Arnulphi
S. Amin-Hanjani
A. Alaraj
M. Zhao
X. Du
S. Ruland
X.J. Zhou
K.R. Thulborn
F.T. Charbel

🔓

BACKGROUND AND PURPOSE: Large-vessel cerebral blood flow quantification has emerged as a potential predictor of stroke risk. QMRA uses phase-contrast techniques to noninvasively measure vessel flows. To evaluate the in vivo accuracy of QMRA for measuring the effects of progressive arterial stenosis, we compared this technique with invasive flow measurements from a sonographic transit-time flow probe in a canine model.

MATERIALS AND METHODS: A sonographic flow probe was implanted around the CCA of hound dogs ($n = 4$) under general anesthesia. Pulsatile blood flow and arterial pressure were continuously recorded during CCA flow measurements with QMRA. A vascular tourniquet was applied around the CCA to produce progressive stenosis and varying flow rates. Statistical comparisons were made by using the Pearson product moment correlation coefficient.

RESULTS: A total of 60 paired CCA flow measurements were compared. Mean blood flows ranged between 21 and 691 mL/min during QMRA acquisition as measured by the flow probe. The correlation coefficients between flow probe and QMRA measurements for mean, maximum, and minimum volume flow rates were 0.99 ($P < .0001$), 0.98 ($P < .0001$), and 0.96 ($P < .0001$), respectively. The overall proportional difference between the 2 techniques was 7.8 ± 1%. Measurements at higher flow rates and in the absence of arterial stenosis had the lowest PD.

CONCLUSIONS: Noninvasive CCA flow measurements by using QMRA are accurate compared with invasive flow-probe measurements in a canine arterial flow model with stenosis and may be useful for the evaluation of the hemodynamic effects of stenosis caused by cerebrovascular atherosclerosis.

ABBREVIATIONS: CCA = common carotid artery; EKG = electrocardiogram; GCFP = global coherent free precession; NOVA = Noninvasive Optimal Vessel Analysis; MRA = MR angiography; PC = phase-contrast; PCMR = phase-contrast MR imaging; PC-VIPR = phase-contrast vastly undersampled isotropic projection; PD = proportional difference; QMRA = quantitative MR angiography; SPECT = single-photon emission CT; TOF = time-of-flight; VENC = velocity-encoding

Cerebral blood flow quantification is an established tool in the evaluation of cerebrovascular diseases and stroke. It can be used to assess the hemodynamic effects of arterial stenosis,[1] evaluate the vasomotor response of an affected cerebral vascular territory,[2] and determine the pattern and volume of collateral circulation to a compromised area.[3]

Noninvasive modalities for assessment of cerebral blood flow include transcranial Doppler, which provides blood flow velocities but is operator-dependent and is limited by anatomic variation (such as vascular tortuosity and skull attenuation), which may prevent insonation in ≤30% of cases.[4] Other techniques such as SPECT,[5] xenon-enhanced CT,[6] positron-emission tomography,[7] CT perfusion,[8] and perfusion MR,[9] have all been used to measure regional cerebral blood flow. In addition to these techniques, which focus on tissue level hemodynamics, assessment of the direct vessel-specific hemodynamic impact of stenotic lesions and their response to interventions such as angioplasty and stent placement has a potentially important role in evaluating patients with cerebrovascular disease.

QMRA is a potential alternative method, which uses PCMR techniques to quantify individual vessel blood flow. However, the accuracy of PCMR can be affected by factors such as partial volume and curved-flow effects. Furthermore, the presence of arterial stenosis can cause complex flow patterns, which result in signal-intensity loss due to intravoxel dephasing and higher order motion encoding. In vitro experiments of PCMR in large vessels have demonstrated the inaccuracies of both velocities and volume flows to be acceptable, at approximately 5%–10%[10]; prior in vivo validation studies have also reported overall good correlation between PCMR and sonography,[11-13] though poor correlation at flows higher than 500 mL/min has been reported.[13] These validation studies were performed in large conduits (aorta artery or 1-inch tubes). Thus, the results may not be applicable to intracranial vessels, given that a decrease of vessel diameter relative to the spatial resolution may affect the accuracy of the volume flow measurements.[14,15] One study examining PCMR accuracy in smaller vessels reported a very favorable PD of 0.8% and a

correlation coefficient of 0.95,[15] but averaging of positive and negative PDs was an analytic flaw resulting in falsely high accuracy. Furthermore, none of these studies used models simulating stenosis in assessing flow accuracy.

The potential for multiple sources of error and time-consuming protocols has previously limited the routine clinical application of PCMR. QMRA offers potential advantages over PCMR alone, by using a 3D rendering of the vasculature with TOF MR angiography for vessel localization and an optimal scan plane determination to reduce partial volume and curved flow effects. The greatest accuracy in PCMR flow measurements is achieved when the imaging plane is perpendicular to the vessel of interest and the VENC is matched to the through-plane flow.[16] The QMRA software has automated the placement of a perpendicular imaging plane and the selection of the appropriate VENC based on the actual flow in the vessel under study. To date, this technique has been used to guide patient management in cerebral revascularization surgery[17-20]; assess intracranial and extracranial vessel stenosis pre- and poststent placement[21]; measure blood flow in cerebral aneurysms[22]; evaluate subclavian steal syndrome[23]; assess collateral volume flow in large-vessel cerebrovascular disease[24]; and predict outcomes of balloon-occlusion testing.[20] Although in vitro validation of QMRA has been performed by using flow phantoms,[16] in vivo evaluation of clinically relevant cerebrovascular flows, in conjunction with progressive arterial stenosis, has not been previously described. In this study, we compared the accuracy of QMRA with the criterion standard for direct flow measurement, the sonographic transit-time flow probe, by using an in vivo canine carotid artery model in which flow rates and degree of stenosis were changed systematically.

Materials and Methods

Animal Preparation

The protocol for this study was reviewed and approved by the Animal Care Committee at University of Illinois at Chicago. All the procedures fulfilled the requirements stated in the *Guide for the Care and Use of Laboratory Animals* (National Academy Press, Washington, DC) and the Animal Welfare Act. Four male hound dogs (weight, 15–20 kg) were used in this study. General anesthesia was induced by using thiopental. Animals were intubated orally, and anesthesia was maintained by using isoflurane (mean alveolar concentration of 1%–3%). The neck was shaved and prepared for a midline neck skin incision to expose the right CCA (Fig 1). The CCA was isolated over a length of 8 cm with no branch vessels in the exposed segment. The diameter of the native CCAs ranged between 2.5 and 3.5 mm. After the CCA was identified, an appropriate-sized sonographic flow probe was placed and secured around the vessel (Fig 1). The space between the vessel and the probe was filled with an acoustic gel to remove as much air from the incision as possible to obtain good sonographic transmission and eliminate magnetic susceptibility artifacts from the MR images. A vascular tourniquet was applied around the CCA to produce varying degrees of stenosis (Fig 1). Four EKG electrodes for cardiac monitoring were applied to the back of the animal to reduce electromagnetic artifacts caused by movement of the leads during the breathing cycle. Arterial blood pressure was continuously monitored and recorded by using a femoral arterial line. The animal was transferred to the MR imaging suite and placed in a supine position inside the MR imaging scanner bore. The anesthesia machine, flowmeter,
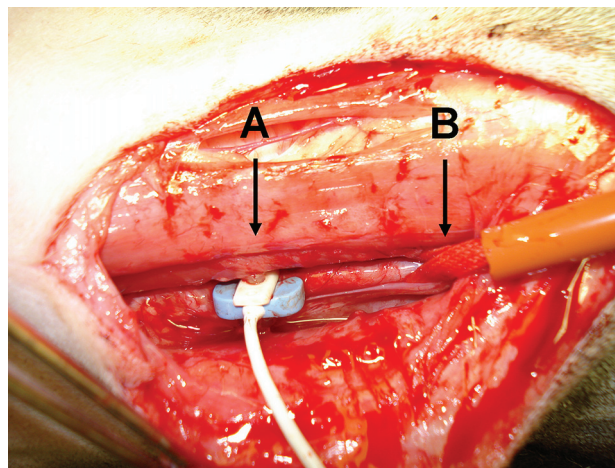

Fig 1. Intraoperative photograph of the dissected CCA of the dog. *A,* Sonographic flow probe around the CCA. *B,* Vascular tourniquet around the CCA.

and blood pressure monitor were placed outside the MR imaging room and connected to the animal inside the magnet by extension tubing, cable, and an arterial line running through a waveguide.

QMRA Flow Measurements

Noninvasive blood flow measurements of the canine CCA were performed by using QMRA. All images were acquired by using a 3T MR imaging scanner (Signa HDx with software Rev 14.0; GE Healthcare, Milwaukee, Wisconsin). A clinical quadrature head coil (GE Healthcare) was used for all image acquisitions. The technique of blood flow quantification by QMRA is described in detail in the Appendix. Horizontally placed plastic tubing with running saline was placed at the level of the probe and used as a dynamic marker during the TOF MRA. The temporal resolution provided by QMRA was 20 data points (phase images) per cardiac cycle, providing a temporal resolution of approximately 50 ms.

Continuous arterial blood pressure and heart rate were recorded by using the arterial femoral line. To produce varying flow rates during the experiment, a vascular tourniquet consisting of a 7-mm-wide vessel band attached to a tightening screw was used to create a variable degrees of stenosis and thus a wide spectrum of blood flows. Flow measurements with QMRA were performed on several CCA segments distal and proximal to the carotid stenosis created by the tourniquet. The location of each measurement with respect to the stenosis was recorded. The mean, maximum, and minimum volumetric blood flows were calculated by NOVA software (VasSol, Chicago, Illinois) on the basis of the entire set of acquired phase images of each QMRA measurement (20 phase images per cardiac cycle during 120 seconds of acquisition time).

Sonographic Blood Flow Measurements

A sonographic transit-time flowmeter (Transonic Systems, Ithaca, New York) with MR imaging−compatible perivascular probes (models 3RB488 and MC2PRB) was used for comparison with QMRA flow measurements. The flow probe uses the principle of sonographic transit time to sense flow in vessels independent of the flow-velocity profile, turbulence, or hematocrit.[25-27] The temporal resolution of the flow probe was 160 Hz. This method provides a temporal resolution of 6.25 ms per measurement, which is several times shorter than the QMRA measurements. This means that instantaneous measurements across the cardiac cycle cannot be compared directly, but rather
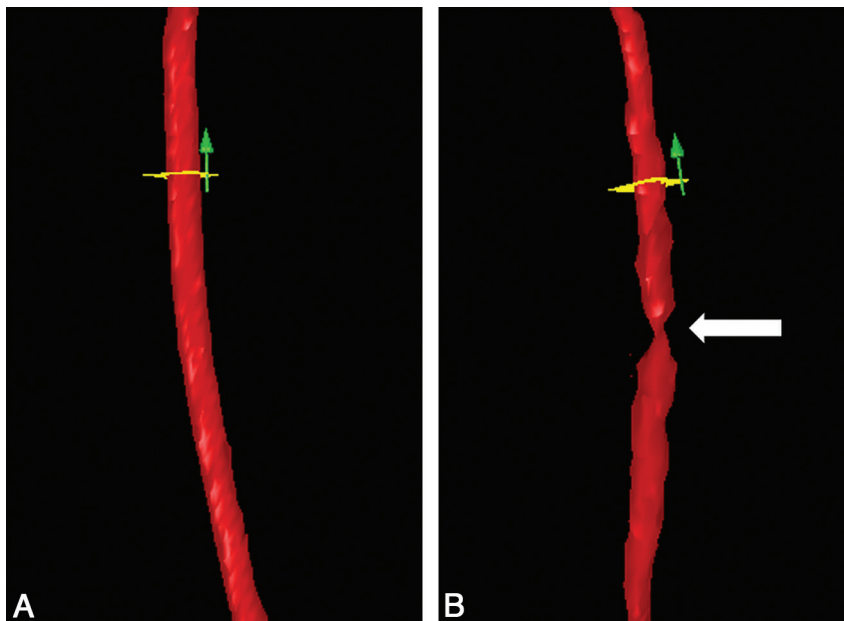
Fig 2. 3D surface rendering of the CCA created by QMRA. *A*: The CCA segment before stenosis is induced. The tourniquet is in place and loose. *B*: The same CCA segment after stenosis is created by tightening the tourniquet. The vertical arrow indicates the direction of flow. The white arrow indicates the position of the stenosis. The flow probe is proximal to the stenosis outside the FOV.

mean measurements across the cardiac cycle can be compared. The instantaneous maximum and minimum flows measured by the probe were expected to be larger and smaller than the QMRA measured flow values, respectively.

Direct blood flow of the canine CCA was measured quantitatively in milliliters per minute by using this sonographic flow-probe device. The accuracy of this probe has already been established in vitro and in vivo.[28,29] Flow velocities, waveforms, and pulse rates were continuously recorded throughout the experiment.

Data Analysis

The QMRA data were processed off-line on a NOVA workstation. The flow rates were interpreted by a blinded reviewer unaware of the animal's flow rates measured by the flow probe. Each QMRA flow measurement was assessed for quality as discussed in the Appendix. Flow measurements meeting these standard criteria were used for analysis.[16] The mean, maximum, and minimum volume flows were tabulated. Sonographic flow measurements were processed off-line to calculate the mean, maximum, and minimum blood flows and heart rates for the equivalent QMRA measurements.

Statistical Analysis

The mean, maximum, and minimum volume flows calculated from QMRA were correlated to the sonographic flow method by using the Pearson product moment correlation coefficient. The comparison of the instantaneous values of the 2 methods is not reasonable due to the different temporal resolutions of the 2 techniques. Because both techniques have their own error of estimation and the true volume flow is unknown, it is not sufficient to compare the in vivo flow estimates via correlation coefficients. Hence, the additional analysis of agreement suggested by Bland and Altman was performed.[30] This consists of plotting the differences between the corresponding sonographic flow probe and QMRA flow estimates as a function of their mean values.

The PD calculated as (Flow Probe − QMRA) / [1/2] (Flow Probe + QMRA) × 100% was used to evaluate disparities between sono-

graphic flow and QMRA flow measurements.[15] The absolute PD was used for statistical calculations. Extreme outliers were identified and excluded by using boxplot statistical techniques (measurements that were 1.5 interquartile ranges higher than the 75th percentile of the dataset).[31] A Student t test was used to compare numeric data. The statistical analysis was performed by using Power Lab Chart 5, Version 5.2.2 (AD Instruments, Bella Vista, New South Wales, Australia) and Microsoft Office Excel 2007 (Microsoft, Bothell, Washington) analysis software.

In an effort to approximate flows of intra- and extracranial arteries in humans, mean flow measurements were categorized into 4 different ranges to reflect flows relevant to various intracranial and extracranial arteries: 10–80 (posterior cerebral artery, anterior cerebral artery), 80–180 (middle cerebral artery, basilar artery), 180–350 (internal carotid artery), and >350 mL/min (ie, the CCA).[32,33] The effect of potential turbulence created by stenosis was evaluated by examining the relative accuracy of flow measurements proximal and distal to the applied tourniquet stenosis.

Results

A series of 79 paired CCA flow measurements, from QMRA and the sonographic flow probe, both with and without stenosis, were analyzed. A 3D surface rendering of axial TOF MRA was used to identify a straight carotid segment with no branches in which flow measurements were performed (Fig 2). Six measurements were excluded as statistical outliers. Thirteen QMRA measurement attempts did not meet routine QMRA acceptability criteria as outlined in the Appendix. All data were accepted or rejected by a blinded reviewer who was not aware of the sonographic flow-probe measurements. Final analysis was, therefore, performed on a total of 60 paired measurements.

The mean flow volume ranged between 21 and 691 mL/min as measured by the invasive sonographic flow probe. The PD between the flow probe and QMRA for mean volume flow
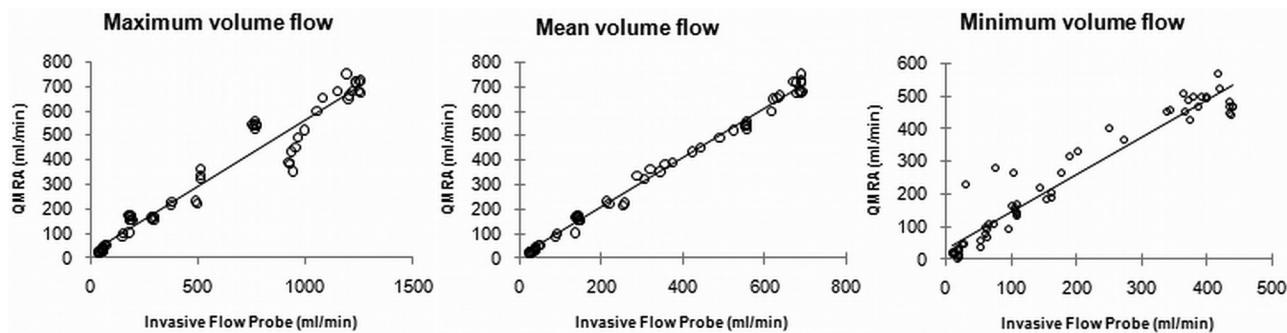
Fig 3. Correlations between mean, maximum, and minimum flow volume rates obtained with QMRA and those obtained with sonographic flow.
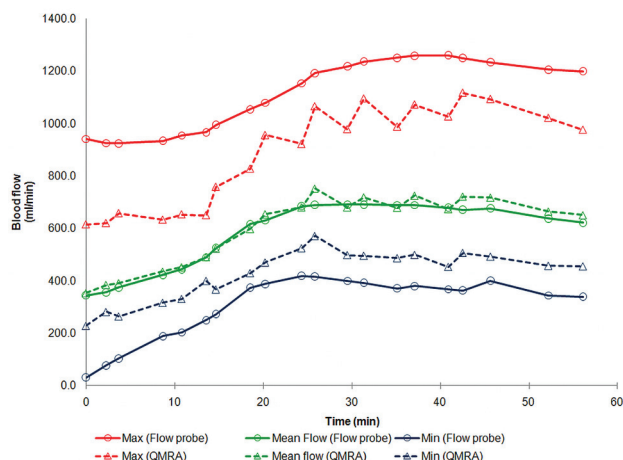

Fig 4. An example of simultaneous flow-volume measurements obtained with QMRA and the flow probe across time in an animal with no stenosis. The QMRA measurements closely track flow-probe measurements for maximum, mean, and minimum flow volumes. The QMRA method gives lower maxima and higher minima compared with the flow probe due to its reduced temporal resolution.

Fig 5. Bland-Altman plot shows the relative degree of agreement between volume flow measurements with QMRA and the invasive flow probe. Dashed lines demonstrate upper and lower limits of agreement. (±2 SDs).

Table 1: Comparison of the PD between flow measurements from QMRA and the flow probe at different flow ranges

Flow (mL/min)	No. of Measurements	PD ($\pm$ SE) (%)	Mean Flow Rate (mL/min)
20–79	13	9.4 $\pm$ 2	34
80–179	14	13.3 $\pm$ 2	134
180–350[a]	8	9.7 $\pm$ 2	274
>350[a]	25	3.2 $\pm$ 0.5	584

[a] Flows obtained without induced stenosis.

was 7.9 $\pm$ 1.0% (SE). High correlation was observed across the broad flow range studied (Fig 3). The correlation coefficient between the flow probe and QMRA for mean volume flow was 0.99 ($P <$ .0001); for maximum volume flow was 0.98 ($P <$ .0001); and for minimum volume flow was 0.96 ($P <$ .0001) (Fig 3). The QMRA measurements closely tracked the measurements obtained with the flow probe in time throughout each experiment (Fig 4).

To investigate agreement between the 2 techniques, we plotted the differences between the corresponding sonographic flow probe and QMRA flow estimates versus their means (including the mean of the differences $\pm$ 2 SDs) by using a Bland-Altman plot (Fig 5). Agreement was found because 97% of the measurements fitted within the limits of agreement (specified as average difference $\pm$ 1.96 SDs of the difference).

The mean flow volume between the 2 techniques was further analyzed across 4 different blood flow ranges. Measurements across subgroups are tabulated in Table 1. Flow measurements performed at >350 mL/min had lower PDs than those performed at 180–350 mL/min ($P =$ .01), 80–179 mL/min ($P =$ .001), and 20–79 mL/min ($P =$ .02).

The accuracy of QMRA for mean volume flows was evaluated relative to the presence of stenosis induced by a tourniquet. Flow values maintained a high degree of correlation for measurements obtained with no stenosis as well as for those
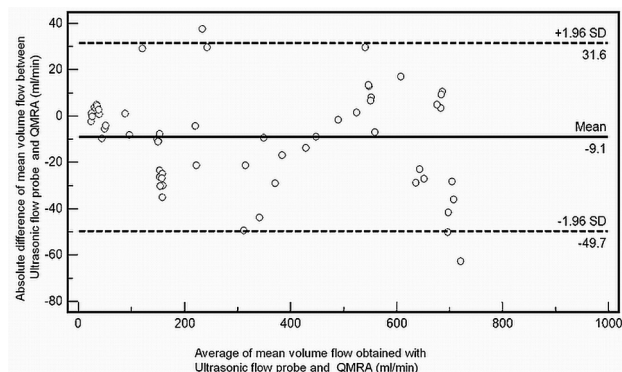
proximal or distal to the stenosis. This correlation was maintained for mean values (Fig 6) and maximum and minimum values (data not shown). Measurements performed without stenosis ($n =$ 33) had statistically lower PDs than measurements performed with stenosis ($n =$ 27, $P <$ .001). The location of the flow measurement proximal to the stenosis had a lower PD than the measurement distal to it, but this was not statistically significant ($P =$ .32) (Table 2).

As noted, the incidence of rejected values in our study was 16.5% (13/79 measurements). Measurements that were obtained in the presence of stenosis had a higher rejection rate (8/40 = 20%) than measurements obtained without stenosis (5/39 = 13%). Within the stenosis subgroup of measurements, there was a higher rejection rate distal to stenosis (7/31 = 22%) versus proximal to it (1/9 = 11%). For rejected values, the calculated flow measurement still provided a reasonable approximation of the actual flow in the absence of stenosis, with an average proportional difference of 8.2% $\pm$ 2 (SE), but a very poor correlation with an average proportional difference of 63.5% $\pm$ 17 (SE) in the presence of stenosis.
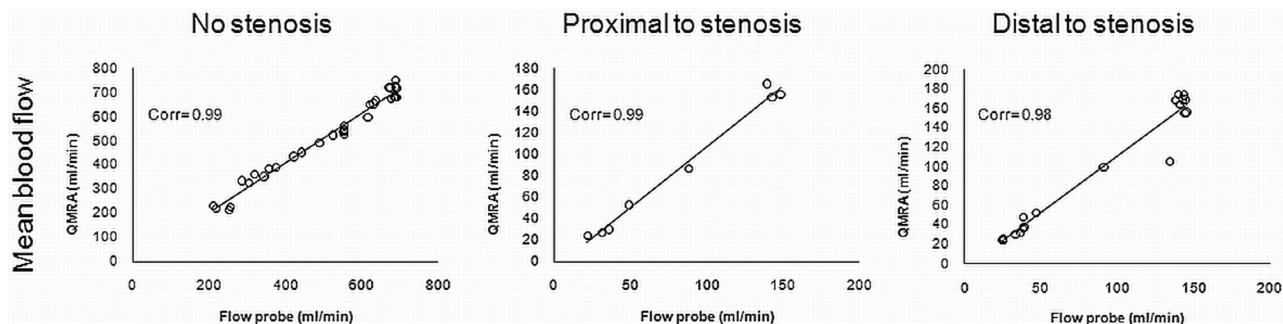
Fig 6. Correlations of mean flow-volume rates between the flow probe and QMRA with no stenosis, proximal to the stenosis, and distal to the stenosis.

Table 2: Comparison of the PD between flow measurements from QMRA and the flow probe across the normal and stenotic CCA as a function of stenosis

Position	PD (± SE) (%)	No. of Measurements	Average Flow (mL/min)
No stenosis	4.8 ± 1	33	509
Stenosis	11.4 ± 1	27	86
Proximal to stenosis	9.6 ± 2	8	82
Distal to stenosis	12.2 ± 2	19	88

Discussion

The purpose of this study was to evaluate the accuracy of QMRA flow measurements in vivo in a small-diameter vessel at different flow ranges induced by varying degrees of stenosis. The overall mean volume flow PD was 7.8 ± 1% (SE) for measurements obtained between 21 and 691 mL/min, showing no significant systematic differences between the 2 methods. Good correlation coefficients for mean, maximum, and minimum flow volumes between the 2 methods were found during the studied flow range.

The in vitro accuracy of the QMRA system has been previously tested by using plexiglass tubes with inner diameters of 6.35 and 4.76 mm.[16] Flow measurements in the phantom showed 7.9% maximum error and an SD of 13 mL/min during pulsatile flow compared with measurements using a sonographic transit-time flowmeter. The percentage difference was higher at lower flow rates: 7.1% at 140 mL/min, 3% at 230 mL/min, and 3.4% at 320 mL/min. Our current in vivo data now indicate that QMRA can be used to measure flows in vessels with a caliber comparable with vessels in the human intracranial circulation with good accuracy. In our study, the sonographic transit-time flow probe was used as the criterion standard comparison because it has been widely used to determine blood flow in small vessels with high accuracy.[28] In vivo validation studies of the flow probe itself have shown a mean error of measurement of 3.4% with coefficients of variation from 2.1% to 4.5%.[29] Several validation studies of flow estimation have used this technique as the criterion standard for flow quantification.[15]

In our experiment, the mean flow volumes were found to be more accurate and had a slightly better correlation coefficient than maximum and minimum flow volumes (Fig 3). This difference can be explained by the different temporal resolutions of the 2 techniques (20 Hz for QMRA versus 160 Hz for the flow probe). Thus, the maximum and minimum points of each cardiac cycle are better defined by the flow probe than by QMRA measurements, which tend to be lower and higher,

respectively, compared with those of the flow probe (Fig 4). However, both techniques still closely track the temporal change in flow across the cardiac cycle. Because mean flow measurements are averaged during the entire cardiac cycle, they serves as a better parameter to compare the 2 techniques. Furthermore, in clinical application, mean flows are relied on rather than maximum or minimum flows.

The accuracy of QMRA was affected, to some degree, by lower flow rates and the presence of induced stenosis. QMRA measurements had lower PDs, indicating better accuracy, at higher flow rates. When analyzing measurements that were obtained without stenosis, higher flow rates (>350 mL/min) had lower PDs (3.2%) than lower flow rates (180–350 mL/min) (PD = 9.7%). The relatively reduced accuracy at lower flow rates has also been observed with in vitro QMRA studies.[16] This phenomenon could be due to the fact that low flow measurements have decreased signal intensity–to-noise ratios due to spin saturation.[34] Flow measurements <180 mL/min were obtained in the presence of stenosis and also demonstrated higher PDs (20–79 mL/min, PD = 9.4%; 80–179 mL/min, PD = 13.3%) (Table 1). The observed change in accuracy for these measurements may reflect not only the effects of reduced flow volume but also the effects of turbulent flow from the stenosis created by the tourniquet.

Measurements performed with no stenosis had lower PDs than measurements performed in the presence of stenosis (Table 2). In addition to the effect of the lower flow rate in the presence of stenosis, this finding could be attributable to stenosis causing complex flow patterns and turbulent jets that result in partial or complete signal-intensity loss. The main mechanisms for this signal-intensity loss include intravoxel dephasing and higher order motion encoding.[35] The higher order motion, such as acceleration, can lead to signal-intensity loss and errors in velocity quantification.[35,36] Intravoxel dephasing is the reduction in the inflow signal-intensity enhancement of moving spins due to phase dispersal within a voxel, resulting in a reduction in the reliability of the measured phase.[35,37] Turbulence is characterized by small-velocity fluctuations superimposed on the principal flow and is commonly associated with the chaotic or irregular motion due to small and large eddies (a current of fluid moving contrary to the principal flow). Signal-intensity loss is dependent on the intensity (size of the fluctuations), scale, and time dependence of the turbulent eddies.[35,38]

We compared measurements placed proximal and distal to the stenosis to determine if there may be a differential accuracy, given that turbulent flow is presumed to be worse down-

stream from the stenosis. Measurements obtained proximal to the stenosis did have lower PDs than those obtained distal to it, but this difference did not achieve statistical significance (Table 2). The small number of measurements proximal to the stenosis ($n = 8$) may have limited the power to detect a difference in our sample. The quality assurance criteria may also have excluded measurements made where there was turbulent flow distal to the stenosis. In our experimental model, vessel stenosis was created artificially by using a vascular tourniquet; this may not accurately reflect the flow patterns or distortions created by atherosclerotic stenosis in the patient setting.[39,40]

A number of flow measurements were discarded because they did not meet the predetermined standard acceptability criteria performed as part of the conventional QMRA protocol (Appendix).[16] To avoid bias in our study, we blinded the reviewer accepting or rejecting QMRA data points to the sonographic flow-probe measurements. The rejection criteria used are regularly applied to QMRA studies done in the clinical setting as well as in the research environment. For clinical studies in humans, the quality-control operation is performed in real-time by the QMRA technician immediately after each flow measurement, allowing the measurement to be repeated if necessary. Each repeated measurement adds only approximately 1 minute of acquisition time to the study.

The rate of rejected values in our study likely reflects strict application of the quality control criteria and the extreme experimental circumstances, such as high degrees of stenosis and extremely low blood flows, tested for purposes of obtaining a full range of results. These findings suggest that turbulent flow contributed not only to lower accuracy, as noted above, but also to higher rejection rates. The underlying causes for PCMR partial or complete signal-intensity loss in the presence of stenosis and turbulent flow have been investigated by other authors, as summarized above, but were beyond the scope of this experiment.

Beyond the standard PCMR and QMRA techniques, other MR imaging techniques such as GCFP MR imaging and PC-VIPR are also being assessed for measuring blood flow. In 1 study of 6 anesthetized dogs, GCFP MR imaging blood flow was found to be linearly related to true blood flow measured by the flow probe ($P < .0001$) and by phase-contrast VENC MR imaging ($P < .0001$)[41]; however, the absolute differences between GCPF and VENC MR imaging to invasive flow-probe measurements were not analyzed. PC-VIPR, a novel 3D MR imaging sequence with potentially better spatial resolution and shorter imaging times than conventional 3D PCMRA, has shown good in vivo and in vitro correlations with 2D cine PCMR flow measurements (correlation coefficient = 0.97).[42] Additionally, several reports have studied the use of this technique to examine pressure gradients across experimental stenosis,[39,43,44] but not blood flow velocities or volumetric flow. Our experiment represents the first in vivo study incorporating stenosis to create a range of blood flows to assess the accuracy of volumetric flow measurements by using PCMR.

Conclusions

Volume flow measurements determined by QMRA in the canine CCA demonstrated overall good accuracy (PD = 7.8%) and good correlation (0.99 correlation coefficient) with direct sonographic transit-time flow measurements during a flow range of 21–610 mL/min. QMRA measurements were feasible in the presence of arterial stenosis. Measurements obtained with no stenosis and at higher flow rates had higher accuracy (PD = 3.2%) than measurements obtained at lower flow rates (PD = 9.6%) and in the presence of arterial stenosis (PD = 11.4%). The accuracy at low flows and in the presence of stenosis was still within ranges that would allow clinical application. QMRA is a promising technique for the evaluation of the hemodynamic effects of cerebrovascular steno-occlusive disease.

Appendix: QMRA Technique

The technique of blood flow quantification by QMRA has been previously described.[16,32] Briefly, QMRA was performed by using the flow-analysis software, NOVA (VassSol). First, 2D and 3D TOF MRA was performed. Acquired images were transmitted to a computer workstation where the NOVA software was used to create a rotating 3D surface rendering of the vasculature by using a marching cube algorithm.[16] From the scan plane calculated by a line-fitting algorithm, a 2D phase contrast cardiac-gated scan was obtained with a double-oblique prescription that was perpendicular to the vessel flow direction. The imaging parameters were as follows: TR, 10–15 ms; TE, 4–7 ms; flip angle, 15; NEX, 4; section thickness, 3 mm; FOV, 180 mm; and matrix, 256 × 192. The EKG signal intensity was used for cardiac gating during QMRA acquisition. A region of interest was automatically placed on the PC images and was also displayed in the 3D surface-rendered image for vessel verification. The area of the vessel was automatically determined. The algorithm for such determination is based on the PCMR property that the phases of stationary tissue pixels are ideally zeros and the phases of moving blood pixels are nonzero. A contour line was drawn by identifying each immediate contiguous voxel with a zero phase value, closing a circle around the vessel. In this manner, isolated voxels with phase noise were not included in the vessel contours. The velocities at all of the pixels inside the vessel border were then integrated to calculate the flow in milliliters per minute. The vessel borders during a cardiac cycle were automatically extracted and displayed on a color-coded and magnified region-of-interest image for vessel-border verification.

The QMRA data had to meet strict NOVA software criteria[16] to be included in final analysis. Each flow measurement was verified for quality on the basis of these criteria, as follows: The phase range used by the QMRA method had to include the maximum flow velocity of the cardiac cycle to avoid aliasing artifacts. If this was not so, the measurement was repeated with a more appropriate maximum velocity by resetting the acquisition parameter, termed VENC, to a different maximum velocity. This step was important because the measured flows were changed throughout the experiment by changing the degree of stenosis. The location of the vessel showing phase changes across the cardiac cycle had to be in the center of the FOV of the double-oblique phase image used to ensure that the flow was perpendicular to the flow direction. This verified that no movement had occurred relative to the 3D TOF angiogram. The spatial profiles of phase and magnitude across the vessel had to be circular and well-defined; these profiles indicated that a true cross-section perpendicular to the vessel had been obtained. The spatial velocity profiles across the vessel

had to show the expected shape with a radial symmetry that registered as rings of increasing velocity from the periphery to the center of the vessel. The temporal flow profile through the cardiac cycle was examined for each measurement to ensure that there was a clearly defined maximum (systole) and minimum (diastole) with a smoothly varying phase change except for the expected small notch between systole and diastole, indicating aortic valve closure. Despite the flow probe continuously monitoring flow during MR imaging and producing some radio-frequency noise across the MR images, the accepted measurements had signal intensity–to-noise ratio and contrast-to-noise ratio performance adequate for high-quality angiography, with excellent background suppression on the 3T scanner used.

QMRA imaging acquisition times in a human head and neck vascular study are as follows: localizer, 6 seconds; head 3D TOF, 9 minutes; neck 2D TOF, 6 minutes; PCMR scanning, 1 minute per measurement; postprocessing time, 1 minute per vessel, with an average total scanning time of 30–45 minutes for the major cervical and intracranial vessels.[32]

Acknowledgments

We thank Lauren Ostergren from VasSol Inc for assisting with literature review and quality control of the flow probe data.

References

1. Wada T, Kodaira K, Fujishiro K, et al. **Correlation of common carotid flow volume measured by ultrasonic quantitative flowmeter with pathological findings.** *Stroke* 1991;22:319–23
2. Levine RL, Turski PA, Turnipseed WD, et al. **Vasodilatory responses and magnetic resonance angiography: extracranial and intracranial intravascular flow data.** *J Neuroimaging* 1997;7:152–58
3. Knappertz VA, Tegeler CH, Myers LG. **Clinical cerebrovascular applications of arterial ultrasound volume flow rate estimates.** *J Neuroimaging* 1996;6:1–7
4. Alexandrov AV, Babikian VL, Adams RJ, et al. **The evolving role of transcranial Doppler in stroke prevention and treatment.** *J Stroke Cerebrovasc Dis* 1998;7:101–04
5. Ogasawara K, Ogawa A, Yoshimoto T. **Cerebrovascular reactivity to acetazolamide and outcome in patients with symptomatic internal carotid or middle cerebral artery occlusion: a xenon-133 single-photon emission computed tomography study.** *Stroke* 2002;33:1857–62
6. Jungreis CA, Yonas H, Firlik AD, et al. **Advanced CT imaging (functional CT).** *Neuroimaging Clin N Am* 1999;9:455–64
7. Pantano P, Baron JC, Lebrun-Grandie P, et al. **Regional cerebral blood flow and oxygen consumption in human aging.** *Stroke* 1984;15:635–41
8. Wintermark M, Thiran JP, Maeder P, et al. **Simultaneous measurement of regional cerebral blood flow by perfusion CT and stable xenon CT: a validation study.** *AJNR Am J Neuroradiol* 2001;22:905–14
9. Butcher K, Parsons M, Allport L, et al. **Rapid assessment of perfusion-diffusion mismatch.** *Stroke* 2008;39:75–81
10. Zananiri FV, Jackson PC, Goddard PR, et al. **An evaluation of the accuracy of flow measurements using magnetic resonance imaging (MRI).** *J Med Eng Technol* 1991;15:170–76
11. Ley S, Unterhinninghofen R, Ley-Zaporozhan J, et al. **Validation of magnetic resonance phase-contrast flow measurements in the main pulmonary artery and aorta using perivascular ultrasound in a large animal model.** *Invest Radiol* 2008;43:421–26
12. Pelc LR, Pelc NJ, Rayhill SC, et al. **Arterial and venous blood flow: noninvasive quantitation with MR imaging.** *Radiology* 1992;185:809–12
13. Pettigrew RI, Dannels W, Galloway JR, et al. **Quantitative phase-flow MR imaging in dogs by using standard sequences: comparison with in vivo flowmeter measurements.** *AJR Am J Roentgenol* 1987;148:411–14
14. Tang C, Blatter DD, Parker DL. **Accuracy of phase-contrast flow measurements in the presence of partial-volume effects.** *J Magn Reson Imaging* 1993;3:377–85
15. Hofman MB, Visser FC, van Rossum AC, et al. **In vivo validation of magnetic resonance blood volume flow measurements with limited spatial resolution in small vessels.** *Magn Reson Med* 1995;33:778–84
16. Zhao M, Charbel FT, Alperin N, et al. **Improved phase-contrast flow quantification by three-dimensional vessel localization.** *Magn Reson Imaging* 2000;18:697–706
17. Ashley WW, Amin-Hanjani S, Alaraj A, et al. **Flow-assisted surgical cerebral revascularization.** *Neurosurg Focus* 2008;24:E20
18. Amin-Hanjani S, Shin JH, Zhao M, et al. **Evaluation of extracranial-intracranial bypass using quantitative magnetic resonance angiography.** *J Neurosurg* 2007;106:291–98
19. Amin-Hanjani S, Du X, Zhao M, et al. **Use of quantitative magnetic resonance angiography to stratify stroke risk in symptomatic vertebrobasilar disease.** *Stroke* 2005;36:1140–45
20. Charbel FT, Zhao M, Amin-Hanjani S, et al. **A patient-specific computer model to predict outcomes of the balloon occlusion test.** *J Neurosurg* 2004;101:977–88
21. Prabhakaran S, Warrior L, Wells KR, et al. **The utility of quantitative magnetic resonance angiography in the assessment of intracranial in-stent stenosis.** *Stroke* 2009;40:991–93
22. Karmonik C, Klucznik R, Benndorf G. **Blood flow in cerebral aneurysms: comparison of phase contrast magnetic resonance and computational fluid dynamics—preliminary experience.** *Rofo* 2008;180:209–15
23. Bauer AM, Amin-Hanjani S, Alaraj A, et al. **Quantitative magnetic resonance angiography in the evaluation of the subclavian steal syndrome: report of 5 patients.** *J Neuroimaging* 2009;19:250–52
24. Ruland S, Ahmed A, Thomas K, et al. **Leptomeningeal collateral volume flow assessed by quantitative magnetic resonance angiography in large-vessel cerebrovascular disease.** *J Neuroimaging* 2009;19:27–30
25. Amin-Hanjani S, Meglio G, Gatto R, et al. **The utility of intraoperative blood flow measurement during aneurysm surgery using an ultrasonic perivascular flow probe.** *Neurosurgery* 2006;58(4 suppl 2):ONS-305–312, discussion ONS-312
26. Amin-Hanjani S, Du X, Mlinarevich N, et al. **The cut flow index: an intraoperative predictor of the success of extracranial-intracranial bypass for occlusive cerebrovascular disease.** *Neurosurgery* 2005;56:75–85, discussion 75–85
27. Charbel FT, Hoffman WE, Misra M, et al. **Ultrasonic perivascular flow probe: technique and application in neurosurgery.** *Neurol Res* 1998;20:439–47
28. Wen C, Li M, Whitworth JA. **Validation of transonic small animal flowmeter for measurement of cardiac output and regional blood flow in the rat.** *J Cardiovasc Pharmacol* 1996;27:482–86
29. Alback A, Makisalo H, Nordin A, et al. **Validity and reproducibility of transit time flowmetry.** *Ann Chir Gynaecol* 1996;85:325–31
30. Bland JM, Altman DG. **Statistical methods for assessing agreement between two methods of clinical measurement.** *Lancet* 1986;1:307–10
31. McGill R, Tukey JW, Larsen WA. **Variations of box plots.** *Am Stat* 1978;32:12–16
32. Zhao M, Amin-Hanjani S, Ruland S, et al. **Regional cerebral blood flow using quantitative MR angiography.** *AJNR Am J Neuroradiol* 2007;28:1470–73
33. Hendrikse J, van Raamt AF, van der Graaf Y, et al. **Distribution of cerebral blood flow in the circle of Willis.** *Radiology* 2005;235:184–89
34. Nasiraei-Moghaddam A, Behrens G, Fatouraee N, et al. **Factors affecting the accuracy of pressure measurements in vascular stenoses from phase-contrast MRI.** *Magn Reson Med* 2004;52:300–09
35. O'Brien KR, Cowan BR, Jain M, et al. **MRI phase contrast velocity and flow errors in turbulent stenotic jets.** *J Magn Reson Imaging* 2008;28:210–18
36. Stahlberg F, Sondergaard L, Thomsen C, et al. **Quantification of complex flow using MR phase imaging: a study of parameters influencing the phase/velocity relation.** *Magn Reson Imaging* 1992;10:13–23
37. Eichenberger AC, Jenni R, von Schulthess GK. **Aortic valve pressure gradients in patients with aortic valve stenosis: quantification with velocity-encoded cine MR imaging.** *AJR Am J Roentgenol* 1993;160:971–77
38. Gatenby JC, Gore JC. **Mapping of turbulent intensity by magnetic resonance imaging.** *J Magn Reson B* 1994;104:119–26

39. Turk AS, Johnson KM, Lum D, et al. **Physiologic and anatomic assessment of a canine carotid artery stenosis model utilizing phase contrast with vastly undersampled isotropic projection imaging.** *AJNR Am J Neuroradiol* 2007;28:111–15

40. Karmonik C, Basto P, Vickers K, et al. **Quantitative segmentation of principal carotid atherosclerotic lesion components by feature space analysis based on multicontrast MRI at 1.5 T.** *IEEE Trans Biomed Eng* 2009;56:352–60

41. Klem I, Rehwald WG, Heitner JF, et al. **Noninvasive assessment of blood flow based on magnetic resonance global coherent free precession.** *Circulation* 2005;111:1033–39

42. Gu T, Korosec FR, Block WF, et al. **PC VIPR: a high-speed 3D phase-contrast method for flow quantification and high-resolution angiography.** *AJNR Am J Neuroradiol* 2005;26:743–49

43. Lum DP, Johnson KM, Paul RK, et al. **Transstenotic pressure gradients: measurement in swine—retrospectively ECG-gated 3D phase-contrast MR angiography versus endovascular pressure-sensing guidewires.** *Radiology* 2007;245:751–60

44. Moftakhar R, Aagaard-Kienitz B, Johnson K, et al. **Noninvasive measurement of intra-aneurysmal pressure and flow pattern using phase contrast with vastly undersampled isotropic projection imaging.** *AJNR Am J Neuroradiol* 2007;28:1710–14